

# Low-power Add-drop Microring Resonator Switch with Positive/negative Phase Tuning using InGaAsP/Si Hybrid MOS Phase Shifter

Yosuke Wakita<sup>(1)</sup>, Rui Tang<sup>(1)</sup>, Hanzhi Tang<sup>(1)</sup>, Shuhei Ohno<sup>(1)</sup>, Tomohiro Akazawa<sup>(1)</sup>, Yuto Miyatake<sup>(1)</sup>,  
Stephane Monfray<sup>(2)</sup>, Frederic Boeuf<sup>(2)</sup>, Kasidit Toprasertpong<sup>(1)</sup>, Shinichi Takagi<sup>(1)</sup>,  
Mitsuru Takenaka<sup>(1)</sup>

<sup>(1)</sup> Department of Electrical Engineering and Information Systems, The University of Tokyo, Japan, [wakita@mosfet.t.u-tokyo.ac.jp](mailto:wakita@mosfet.t.u-tokyo.ac.jp)

<sup>(2)</sup> STMicroelectronics, France

**Abstract** We demonstrated add-drop Si microring resonator switch using InGaAsP/Si hybrid MOS optical phase shifter. Through careful Si waveguide design, quasi-single-mode add-drop operation with bipolar phase tuning was achieved. Owing to negligible gate leakage current, high extinction ratio of 34 dB was obtained with 150 fW. ©2023 The Author(s)

## Introduction

Si Programmable photonic integrated circuits (PICs) are emerging to process signals in the optical domain for communication, computing, and sensing [1-3]. For deep learning, we have proposed a ring resonator crossbar array that enables on-chip learning and inference [4, 5]. In the previous demonstration, we have found thermal crosstalk caused by thermo-optic (TO) phase shifters has been a major issue; thus, we have instead proposed to use a III-V/Si hybrid metal-oxide-semiconductor (MOS) optical phase shifter with extremely low power consumption because electron accumulation at the III-V MOS interface enable the large carrier-induced refractive index change [6, 7]. Although hybrid MOS optical phase shifters using ultra-thin InP on a single-bus Si ring resonator have been successfully demonstrated [8], an add-drop Si microring resonator with a hybrid MOS optical phase shifter, which is necessary for the proposed microring crossbar array, has not yet been demonstrated. While the use of 25-nm-thick InP membrane enables the simple integration, there are still issues such as low modulation efficiency and the inability to perform reverse bias operation for positive/negative phase tuning.

In this paper, we integrate a III-V/Si hybrid optical phase shifter on an add-drop Si ring resonator using a 200-nm-thick InGaAsP membrane to overcome the issues in a 25-nm-thick InP membrane. Using a 200-nm-thick InGaAsP layer instead of a 25-nm-thick InP layer results in an increased phase tuning range due to the higher modulation efficiency and the ability to operate under forward and reverse bias. We discuss the design of an appropriate Si waveguide to integrate a 200-nm-thick InGaAsP membrane disk on a Si microring resonator, which enables a quasi-single-mode resonance.

As a result, we successfully demonstrated an add-drop ring resonator switch operation. Compared to an InP membrane, the phase tuning range was extended by a factor of 18. Moreover, the switching energy at 6 V bias was less than 150 fW owing to the small gate leakage current.

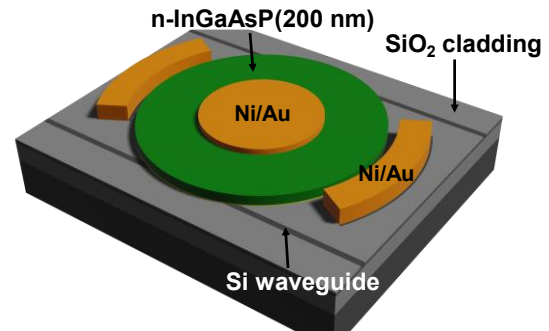


**Fig. 1:** Schematic of add-drop microring resonator switch with III-V/Si hybrid MOS phase shifter.

## Device design

Figure 1 shows a schematic of an add-drop Si microring resonator switch with a III-V/Si hybrid MOS phase shifter where a 200-nm-thick n-InGaAsP membrane is bonded upon a p-Si waveguide with Al<sub>2</sub>O<sub>3</sub> gate dielectric. When a thick III-V membrane is used, there are several optical modes in the structure of the Si waveguide with a III-V disk. To ensure a quasi-single-mode resonance, it is necessary to carefully design a Si waveguide. In this paper, we examined two types of Si waveguides: shallow rib and deep rib waveguides on a 300-nm-thick Si-on-insulator (SOI) wafer, as shown in Fig. 2. The mesas of the shallow rib waveguide and deep rib waveguide have slab heights of 160 nm and 50 nm, respectively. To ensure single-mode operation in Si waveguides, we set the widths of the waveguides to 450 nm and 360 nm, respectively.

We have performed optical mode analysis of

Si ring waveguides with a 200-nm-thick InGaAsP membrane as a function of the radius using Lumerical MODE Solutions. To avoid the sidewall scattering of the edge of the InGaAsP membrane, the radius of InGaAsP disk was designed to be 1  $\mu\text{m}$  larger than that of the Si ring. Figures 2a and 2b show the round-trip optical loss of fundamental and first-order transverse electric (TE) modes in the shallow and deep rib hybrid waveguides, respectively. In the case of the shallow rib waveguide, the first-order TE mode exhibits a large optical loss because of the weak optical confinement. Therefore, the higher-order modes decay while propagating in the ring waveguide, and the ring resonator can be considered to operate as a quasi-single mode. In contrast, in the case of the deep rib waveguide, both TE modes have negligible loss because of the strong optical confinement in the hybrid waveguide or the InGaAsP disk. Therefore, it can be considered that multiple resonant peaks are observed when analysing the spectrum of the ring resonator.

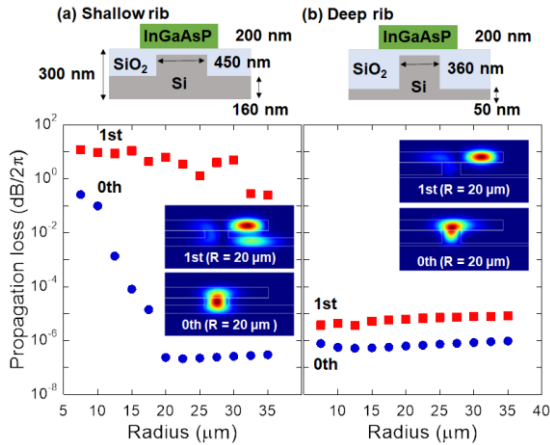
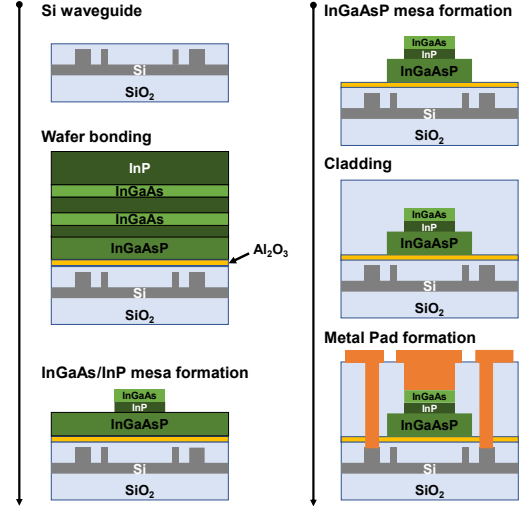


**Fig. 2:** Optical loss of TE modes as a function of radius in (a) shallow rib waveguide (b) deep rib waveguide.

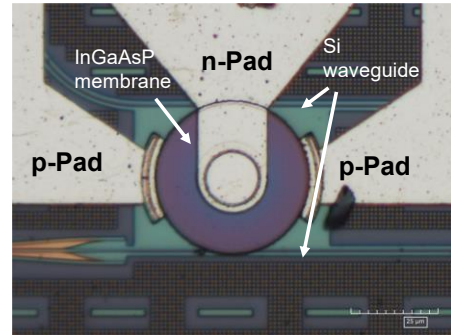
### Device Fabrication

According to the numerical analysis, we have fabricated an add-drop Si microring resonator switch with a III-V/Si hybrid MOS optical phase shifter using the shallow and deep rib Si waveguides. Figure 3 shows the fabrication procedure. After fabricating Si waveguides and grating couplers for a 1550 nm wavelength on a 300-nm-thick SOI wafer, a  $\text{SiO}_2$  cladding layer was deposited and planarized by CMP. The thickness of the  $\text{SiO}_2$  layer was approximately 8 nm. An InP epitaxial wafer containing a 200-nm-thick n-InGaAsP layer was bonded onto a Si rib waveguide via  $\text{Al}_2\text{O}_3$ . The total  $\text{Al}_2\text{O}_3$  thickness was 10 nm. After removal of the InP substrate and etch-stop layers, a disk-shaped InGaAsP mesa with an InGaAs contact layer was formed on the Si ring resonator by electron beam (EB)

lithography and dry etching. After the  $\text{SiO}_2$  cladding layer was deposited by PECVD, Ni/Au was deposited using EB evaporator, and the electrodes were formed by lift-off. Figure 4 shows a plan-view microscopy image of the fabricated device.



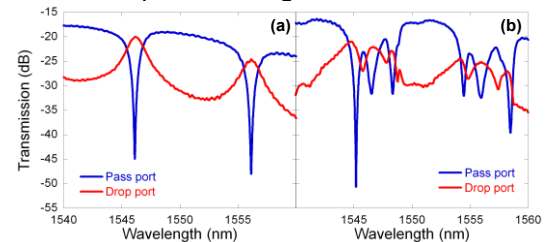
**Fig. 3:** Fabrication procedure of III-V/Si hybrid MOS optical phase shifter.



**Fig. 4:** Microscopy image of fabricated III-V/Si hybrid MOS optical phase shifter on add-drop ring resonator.

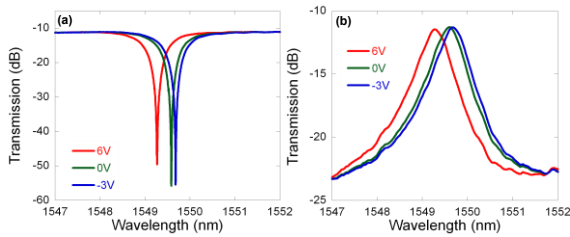
### Measurement

We measured the add-drop ring resonator with III-V/Si hybrid MOS optical phase shifter. Figure 5 shows the output spectra of the pass and drop ports when the radius of the microring is 10  $\mu\text{m}$ . It is found in Fig. 5 that the shallow rib waveguide exhibits a single resonance peak, whereas the deep rib waveguide exhibits multiple resonance peaks, as expected in Fig. 2.



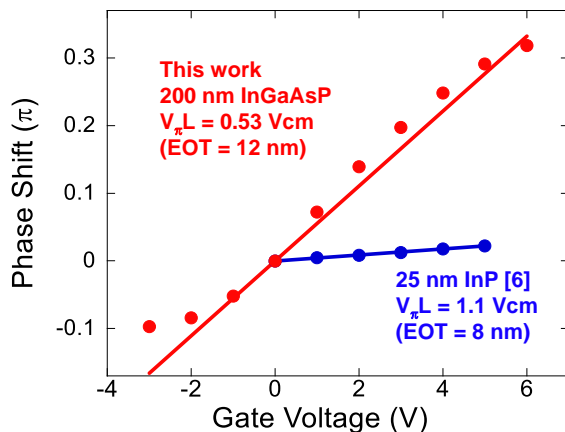
**Fig. 5:** The output spectra of ring resonator with III-V/Si hybrid MOS optical phase shifter in the case of (a) shallow rib waveguide and (b) deep rib waveguide.

Then, a gate voltage was applied between the InGaAsP disk and Si waveguide to measure the phase modulation characteristics of the III-V/Si hybrid MOS optical phase shifter. Figure 6 shows the measured output spectra for the pass port and drop port. By using a 200-nm-thick InGaAsP membrane, we were able to achieve a phase shift not only when a positive gate voltage was applied (carrier accumulation), but also when a negative gate voltage was applied (the Franz-Keldysh effect). As a result, we achieved an add-drop operation with positive/negative phase tuning by the InGaAsP/Si hybrid MOS phase shifter. Owing to the low-loss phase modulation, the high extinction ratio of 34 dB in the pass port was achieved when  $V_g$  was changed from 0 V to 6 V. Note that the extinction ratio in the drop port can be improved by optimizing the initial coupling ratio between the bus and ring waveguides.



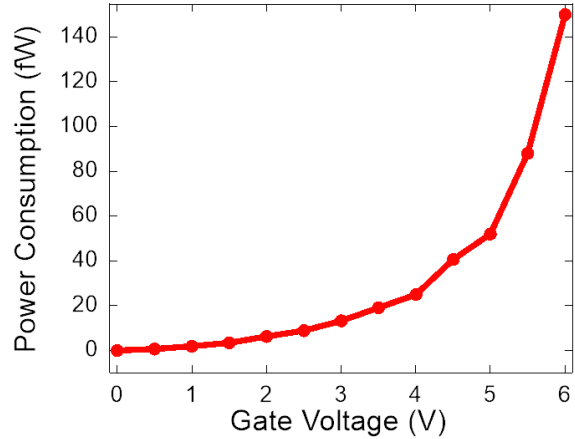
**Fig. 6:** The output spectra of the (a) pass port and (b) drop port as a function of gate voltage  $V_g$ .

Figure 7 shows the phase shift of the III-V/Si hybrid MOS optical phase shifter as a function of  $V_g$ . For comparison, the phase shift in the case of a 25-nm-thick InP membrane [6] was also plotted. The modulation efficiency of the phase shifter was found to be 0.53 Vcm, which is approximately two times better than that of InP membrane. In conjunction with the ability of the positive/negative phase tuning owing to the thick InGaAsP membrane, compared to the InP membrane, the phase tuning range was extended by a factor of 18, even with the thicker equivalent gate oxide thickness (EOT).



**Fig. 7:** Phase shift of the III-V/Si hybrid MOS optical phase shifter as a function of gate voltage.

Figure 8 shows the power consumption of the III-V/Si hybrid MOS optical phase shifter. Although the gate leakage current increases as  $V_g$  increases, we achieved an extremely low static power consumption of approximately 150 fW, when  $V_g$  was 6 V, which is almost 10th orders of magnitude lower than that of a TO phase shifter.



**Fig. 8:** Power consumption of the III-V/Si hybrid MOS optical phase shifter.

## Conclusions

We successfully demonstrated an add-drop microring resonator switch using III-V/Si hybrid MOS optical phase shifter. Through the careful consideration in a Si waveguide design, we achieved a quasi-single-mode operation in the add-drop operation even using a 200-nm-thick InGaAsP membrane. In conjunction with a high modulation efficiency and bipolar phase tuning, the phase tuning range of the III-V/Si hybrid MOS phase shifter with a 200-nm-thick InGaAsP membrane was 18 times greater than that with a 25-nm-thick InP membrane. As a result, the high extinction ratio of 34 dB was obtained at 6 V gate voltage with an extremely low static power consumption of 150 fW. Thus, the demonstrated add-drop microring resonator switch is in particular suitable for a microring crossbar circuit for communication and computing.

## Acknowledgements

This work was partly supported by JST-Mirai Program (JPMJMI20A1), JST, CREST (JPMJCR2004), JSPS KAKENHI (JP23H00172), and ARIM of MEXT under Proposal Number JPMXP1222UT1028, and partly based on results obtained from project (JPNP16007) commissioned by NEDO. The authors thank Dr. H. Yagi, Dr. Y. Itoh, and Dr. H. Mori of Sumitomo Electric for providing InP epitaxial wafers.

## References

- [1] W. Bogaerts, D. Pérez, J. Capmany, D. A. B. Miller, J. Poon, D. Englund, F. Morichetti, and A. Melloni, "Programmable photonic circuits," *Nature*, vol. 586, no. 7828, pp. 207–216, 2020, DOI: [10.1038/s41586-020-2764-0](https://doi.org/10.1038/s41586-020-2764-0).
- [2] Y. Shen, N. C. Harris, S. Skirlo, M. Prabhu, T. Baehr-Jones, M. Hochberg, X. Sun, S. Zhao, H. Larochelle, D. Englund, and M. Soljačić, "Deep learning with coherent nanophotonic circuits," *Nature Photonics*, vol. 11, no. 7, pp. 441–446, 2017, DOI: [10.1038/nphoton.2017.93](https://doi.org/10.1038/nphoton.2017.93).
- [3] R. Tang, M. Okano, K. Toprasertpong, S. Takagi, D. Englund, and M. Takenaka, "Two-layer integrated photonic architectures with multiport photodetectors for high-fidelity and energy-efficient matrix multiplications," *Opt. Express*, vol. 30, no. 19, pp. 33940–33954, 2022, DOI: [10.1364/OE.457258](https://doi.org/10.1364/OE.457258).
- [4] S. Ohno, K. Toprasertpong, S. Takagi, and M. Takenaka, "Si microring resonator crossbar arrays for deep learning accelerator," *Jpn. J. Appl. Phys.*, vol. 59, SGGE04, 2020, DOI: [10.35848/1347-4065/ab6d82](https://doi.org/10.35848/1347-4065/ab6d82).
- [5] S. Ohno, R. Tang, K. Toprasertpong, S. Takagi, and M. Takenaka, "Si Microring Resonator Crossbar Array for On-Chip Inference and Training of the Optical Neural Network," *ACS Photonics*, vol. 9, no. 8, pp. 2614–2622, 2022, DOI: [10.1021/acsp Photonics.1c01777](https://doi.org/10.1021/acsp Photonics.1c01777).
- [6] J. H. Han, F. Boeuf, J. Fujikata, S. Takahashi, S. Takagi, and M. Takenaka, "Efficient low-loss InGaAsP/Si hybrid MOS optical modulator," *Nature Photonics*, vol. 11, no. 8, pp. 486–490, 2017, DOI: [10.1038/nphoton.2017.122](https://doi.org/10.1038/nphoton.2017.122).
- [7] M. Takenaka, J. H. Han, F. Boeuf, J. K. Park, Q. Li, C. P. Ho, D. Lyu, S. Ohno, J. Fujikata, S. Takahashi, and S. Takagi, "III–V/Si Hybrid MOS Optical Phase Shifter for Si Photonic Integrated Circuits," *J. Lightwave Technol.*, vol. 37, no. 5, pp. 1474–1483, 2019, DOI: [10.1109/JLT.2019.2892752](https://doi.org/10.1109/JLT.2019.2892752).
- [8] S. Ohno, Q. Li, N. Sekine, H. Tang, S. Monfray, F. Boeuf, K. Toprasertpong, S. Takagi, and M. Takenaka, "Si microring resonator optical switch based on optical phase shifter with ultrathin-InP/Si hybrid metal-oxide-semiconductor capacitor," *Opt. Express*, vol. 29, no. 12, pp. 18502–18511, 2021, DOI: [10.1364/OE.424963](https://doi.org/10.1364/OE.424963).